

Final Report—Task 6.0.2
Covering the Period 1 October 1988 to 30 September 1989

December 1989

OBSERVATION OF NEUROMAGNETIC FIELDS IN RESPONSE TO REMOTE STIMULI

Prepared By: Edwin C. May
Wanda W. Luke
Virginia V. Trask
Thane J. Frivold

Prepared for:

SG1J

Contracting Officer's Technical Representative
SRI Project 1291

Approved by:

MURRAY J. BARON, Director
Geoscience and Engineering Center



SRI International

This document is made available through the declassification efforts
and research of John Greenewald, Jr., creator of:

The Black Vault



The Black Vault is the largest online Freedom of Information Act (FOIA)
document clearinghouse in the world. The research efforts here are
responsible for the declassification of hundreds of thousands of pages
released by the U.S. Government & Military.

Discover the Truth at: **<http://www.theblackvault.com>**

ABSTRACT

During FY 1989, we conducted a successful, conceptual replication of an SRI/Langley Porter study in which a single subject's central nervous system (CNS) responded to a remote, and isolated flashing light. The CNS activity of eight remote viewers was monitored by a seven-channel magnetoencephalograph (MEG). Visual stimuli were randomly presented to an isolated individual who acted as a "sender" while MEG data were collected from a viewer. These were 5-cm square, linear, vertical, sinusoidal grating lasting 100 ms (remote stimuli). Time markers were randomly indicated in the data stream as control periods (pseudo stimuli). The dependent variable was the RMS average phase shift (resulting from the remote stimuli) of the dominant alpha frequency. Using a Monte Carlo technique to estimate p-values, we observed statistical evidence that the relative phase shift from -0.5 to 0.5 seconds of a remote stimulus are *not* characteristic of the data at large ($Z_s = 1.99, p \leq 0.024, effect\ size = 0.599$). Similarly, the combined statistic for a control stimulus indicates that the relative phase shift from -0.5 to 0.5 seconds of a control stimulus are also *not* characteristic of the data at large ($Z_s = 2.92, p \leq 0.002, effect\ size = 0.924$). Averaged across all viewers, the magnitude of the results, as indicated by the effect sizes of 0.599 and 0.924, respectively, is considered robust by accepted behavioral criteria defined by Cohen. This result was unexpected, and suggests that we may have observed a CNS response to an unintended stimulus (i.e., electromagnetic interference, EMI, from the computing hardware). However, in the SRI/Langley Porter study, EMI had been eliminated, thus, it remains possible that the CNS changes resulted from an anomalous form of information transfer.

TABLE OF CONTENTS

ABSTRACT	ii
LIST OF TABLES	iv
LIST OF FIGURES	iv
I INTRODUCTION	1
A. History of Physiological Correlates to Psychoenergetic Functioning	1
B. Technological Background	2
II METHOD OF APPROACH	5
A. General Description	5
B. Protocol	5
C. Data Analyses	9
D. Monte Carlo Calculations	10
III RESULTS	11
A. Calculations	11
B. Monte Carlo Estimates of Significance	19
C. Results: Button Presses	20
IV DISCUSSION AND CONCLUSIONS	22
A. Root-Mean-Square Phase	22
B. Viewer Dependencies	26
C. Pseudo Stimuli	26
D. Recommendations for Further Research	29
V ACKNOWLEDGMENT	30

LIST OF TABLES

1. Results of Monte Carlo Calculation for RMS Phase	20
2. Data Schema for Interval Conditions	21
3. Button Pressing Results	21
4. Comparison Between Monte Carlo Phases and Theory	24

LIST OF FIGURES

1. Schematic Timing Protocol—Single Run	7
2. Sensor Position Relative to the Inion (0,0) for Viewer 002	8
3. Idealized Results for a Single Stimulus	9
4. Viewer 2: Date 8/25/88: Session 1: Time Average	12
5. Viewer 2: Date 8/25/88: Session 1: Power Spectra of Time Average (RS)	13
6. Viewer 2: Date 8/25/88: Session 1: Average Power Spectra (RS)	13
7. Viewer 2: Date 8/25/88: Session 1: Average Power Gain (RS)	14
8. Viewer 2: Date 8/25/88: Session 1: RMS Phase (RS)	15
9. Viewer 2: Date 8/25/88: Session 1: Time Average (PS)	16
10. Viewer 2: Date 8/25/88: Session 1: Power Spectra of Time Average (PS)	16
11. Viewer 2: Date 8/25/88: Session 1: Average Power Spectra (PS)	17
12. Viewer 2: Date 8/25/88: Session 1: Average Power Gain (PS)	17
13. Viewer 2: Date 8/25/88: Session 1: RMS Phase (PS)	18
14. Viewer 2: Date 8/25/88: Session 1: RMS Phase Difference (RS-PS)	18
15. Viewer 2: Date 8/25/88: Session 1: RMS Phase: Sensor: 2: RS = 118	19
16. Idealize Distributions for Relative Phase Shifts	23
17. Phase Distributions for Viewer 002: 8/25/88	25
18. Phase Distributions for Viewer 007: 3/29/89	25
19. Phase p-values for Viewer 002: 8/25/88	26
20. Sequence of Events for Stimuli Generation	27

I INTRODUCTION

A. History of Physiological Correlates to Psychoenergetic Functioning

Evidence from several laboratories has indicated the possible existence of an as-yet-unidentified channel wherein information is coupled from remote electromagnetic stimuli to the human nervous system. Usually, the coupling has been indicated by physiological responses, even though there was no evidence of cognitive awareness of these stimuli. Physiological measures have included a plethysmographic response^{1*} and electroencephalogram (EEG) activity.^{2,3} Kamiya, Lindsley, Pribram, Silverman, Walter, and others have suggested that the whole range of EEG activity, including evoked potentials, spontaneous EEG, and the contingent negative variation (CNV) might be sensitive indicators of responses to remote stimuli.⁴

In 1974, SRI International conducted a pilot study that investigated a single remote viewer's central nervous system (CNS) response to a remote light stimulus.⁵ In this experiment, the viewer was asked to focus attention on a remote flashing (16-hertz [Hz]) light. Control periods (no light flashing) were randomly mixed with effort periods (light flashing). The viewer was further asked to register when he† perceived the flashing light by pressing a button.

During this pilot experiment, the viewer showed a significant‡ decrease in alpha production when the remote light was flashing, compared with when the light was off. His button presses were random, however, indicating he was not cognitively aware of the flashing light. Two replications of this experiment were conducted with the same viewer at Langley Porter Neuropsychiatric Institute in San Francisco by Drs. David Galin and Robert Ornstein.⁶ In the first of two experiments, the viewer continued to show a significant decrease of occipital alpha production only under the remote flashing light condition. In a second experiment conducted 3 months later, however, the viewer demonstrated a significant increase of occipital alpha production.

Although we found that significant correlations appear to exist between the times of light flashes and CNS activity, we consider this result to be only suggestive, with a definitive conclusion requiring further experimentation.

With the advent of more sensitive CNS monitoring equipment, known as magnetoencephalography (MEG), and with an additional 15 years of remote viewing experience,

* References are at the end of this report.

† To keep the identity of the viewers confidential, we use the pronouns *he* and *his* throughout this report, regardless of the viewer's gender.

‡ Throughout this report, the word "significant" conforms to the standard definition; $p \leq 0.05$.

SRI conducted an experiment to explore possible correlations between CNS activity and remote stimuli. This experiment is the subject of this report.*

B. Technological Background

Magnetoencephalography is a noninvasive technique used to measure, in three-dimensional space, magnetic fields produced by neuronal electric currents in the cortex of the brain. A magnetoencephalography device (MEG) can determine the spatial distributions of specific groups of neurons participating in a given activity and their patterns of activity over time. This technology has been used in research ranging from evaluating how normal brains process information to diagnosing clinical conditions such as epilepsy and dementias.⁷

Neurons that participate in a given functional activity communicate between themselves and ultimately other parts of the body by electrical signals. These signals are produced by a flow of sodium, chlorine, potassium, and calcium ions traveling from the dendrites down the axon and to the synaptic buttons of each neuron. Such neurons may act as a magnetic dipole that produces a magnetic field.

The sensing device of a MEG is a cryogenic superconducting quantum interference device (SQUID) coupled with a gradiometer. SQUIDS currently being used are cooled by liquid helium. At a few degrees above absolute zero, an electrical current can flow through a superconductor with no applied voltage. "The material of the SQUID consists of superconducting loops with two sections of thin insulating material connecting them (Josephson Junctions). This configuration is referred to as a DC SQUID. Some electrons can tunnel through this insulation. The presence of a weak magnetic field produces a phase difference for the wave function of the magnetic field [and] produces a phase difference for the wave function of the electrons across this barrier. The resulting interference pattern produced by the two different wave functions on each side of the barrier can be used to indicate the strength of these extremely weak magnetic fields."[†]

The neuronal magnetic fields from the human brain are only about 10^{-13} tesla, while the earth's magnetic field is 10^{-4} tesla and normal urban noise is about 10^{-7} tesla. Care must be taken, therefore, to assure that the signal-to-noise ratio is favorable. This has been taken into consideration by the manufacturer of MEG equipment (BTi of San Diego, California), who has designed highly shielded sensors that use a second-order coupled gradiometer to reduce the environmental noise by about 10^6 . The use of an aluminum and μ -metal magnetically shielded room can further reduce the noise by a factor of 10^3 . If used together, these two precautionary

* This report constitutes the deliverable for fiscal year 1989 Statement of Work, item 6.0.2.

† We thank Dr. Edward Flynn, Neuromagnetism Laboratory, Life Science and Physics Division, Los Alamos National Laboratory, Los Alamos, New Mexico, for providing this explanation.

measures can reduce the ambient noise by a factor of about 10^9 —equivalent to the internal SQUID noise.

Because a MEG responds best to neuronal currents that are parallel to the skull (i.e., currents producing magnetic fields oriented tangentially to the skull), neuronal currents perpendicular to the skull may be missed. In reality, however, few neuronal electrical currents are exactly perpendicular to the skull, so some tangential component is almost always available to the SQUID.

Searching for a closely packed group of neurons can be a slow and tedious process. Due to technological restraints, a maximum of seven sensors can be used simultaneously to gather MEG measurements. Sensors on a seven-channel MEG are located on a 2-cm equilateral triangular grid forming the center and vertices of a regular hexagon. A subject wears a spandex cap with grid marks lined up with his nasion, inion, and earlobes to serve as a head-centered coordinate system. To identify the location of a neuronal-equivalent current dipole, many measurements have to be taken. Isocontour maps of field strength are used to represent the amplitude and polarity distribution of the magnetic fields. A least-squares procedure is applied to the observed fields to estimate the location of neuronal sources and orientation of the equivalent current dipole.⁸ The estimated location of the neuronal source can then be identified anatomically with a magnetic resonance image scan of the head. Developments in technology may soon allow for enough channels to cover the whole head at once, thereby reducing data collection time and increasing precision.

MEG technology is based on a cryogenic SQUID operating in liquid helium. Because the Dewar flask cannot exceed a 45-degree angle, subjects must lie prone beneath the apparatus. MEG sensors are not attached to the head, but are lowered into position over the skull; the subject cannot move his head during monitoring without disturbing the measurement. For these two reasons, MEG equipment is not suited for long-term monitoring of a subject. These problems may be solved in the near future as new technology, such as high-temperature SQUIDS, develops.

A response from the MEG is a complex waveform consisting of a series of negative and positive peaks or components. Specific components of this waveform can be correlated with perceptual and cognitive processes. The most commonly observed response to a visual or auditory stimulus, for example, is a large component occurring approximately 100 ms after the onset of the stimulus. One hundred milliseconds appears to be the average latency period between stimulus and the first correlated neuronal activation in the brain.⁸

The earlier EEG technology measures electric potential, or event-related potentials (ERPs) produced by the electrical activity of the brain. A MEG measures the magnetic fields, or event-related fields (ERFs) produced by the electrical activity of specific groups of active neurons in the cortex. An EEG and a MEG, therefore, reveal different aspects of the electrical activity of

the brain and are often used as complementary technologies. In some areas, however, the MEG technique has definite advantages over the EEG:

- (1) ERPs taken from the scalp provide little information regarding the precise three-dimensional distribution of the neuronal sites producing the electrical activity. Brain tissues of unknown electrical conductivity and thickness, individual variations in skull thickness and geometry, and proximity to openings in the skull all make obtaining such detailed information difficult. The same is not true when using a MEG. Neuronal magnetic fields can travel through brain tissues without being significantly altered; this property, coupled with the dipole model, results in high spatial resolution of the neuronal activity.
- (2) EEG procedures are occasionally costly and can be invasive: EEG electrodes must be attached directly to the skull or to the brain of the subject, whereas MEG sensors are extracranial and are simply lowered into position against the skull.
- (3) There is much controversy over the appropriate reference electrode in EEG work (a reference electrode is required with electric potential measurements, because only differences in electric potential are measured). There is no such problem with a MEG, because the measurement of magnetic fields is absolute.

In a cooperative arrangement with Los Alamos National Laboratory (LANL), we have been provided access to a seven-channel MEG under the auspices of the Neuromagnetism Laboratory.

II METHODS OF APPROACH

Our goal was to conduct a conceptual replication of the earlier SRI/Langley Porter experiments. Our basic hypothesis is that a viewer's CNS would respond to a remote light stimulus.

A. General Description

Using a seven-sensor MEG in a shielded room, we investigated the occipital-cortex neuronal magnetic activity that might occur in response to a remote "visual" stimulus.

The following definitions may be helpful:

- Viewer—An individual who attempts extrasensorimotor communication with the environment (e.g., the perception of remote stimuli).
- Direct Stimuli (DS)—Visual stimuli occurring within the normal visual sensory channels.
- Sender—An individual who, while receiving direct stimuli, acts as a putative transmitter to a remote individual (i.e., viewer) who is attempting to receive the same information via extrasensorimotor communication.
- Remote Stimuli (RS)—Visual stimuli occurring outside the normal range of known sensory channels.
- Pseudo Stimuli (PS)—A time marker in the data stream with no associated stimuli.

In this report, a direct stimulus to the sender is also considered as an remote stimulus to the viewer.

B. Protocol

1. General Considerations

To begin a session, a sender is isolated in a room while a viewer is monitored by a MEG in a shielded room about 40 m away. Only the sender is presented with a number of direct visual stimuli at random intervals within a 120-second period, the length of one run. One session usually consists of 10 runs.

a. Viewers

Eight viewers were selected for this experiment. Four were known to be good remote viewers, and four were staff members with unknown viewing ability. Each viewer contributed a minimum of one and a maximum of three independent sessions.

b. Senders

The senders in all sessions were either various staff members who were well known to the viewers or they were viewer's spouses.

c. Dependent Variable

The dependent variable is the RMS phase shift of the primary alpha activity as a result averaged over all RS.

2. Specific Protocol Details

a. Stimuli

Remote stimuli consisted of an NTSC encoded blank screen with a 5-cm square, linear, vertical, sinusoidal grating lasting about 100 ms. These stimuli (DS to the sender) subtended 2 degrees in the lower left visual field of the sender. This was maintained by asking the sender to focus his visual attention on a permanent mark on the monitor. Pseudo stimuli consisted of the blank screen without the superimposed grating, and were included as a putative within-run control.

b. Run Timing

Figure 1 shows a schematic timing diagram for one run. No two stimuli of any type were allowed to occur within a 3-second period of each other. A stimulus may occur, however, any time within a 4.5-second window thereafter. The sender was presented with a minimum of 9 and a maximum of 15 DS occurring at random intervals within a 120-second period. In all but the first session, a random number of pseudo stimuli (i.e., random time markers with no concomitant stimuli—PS) were added as a within-run control. A viewer was never presented with direct stimuli except in locating the maximal response to the visual areas (see Section 2.c).

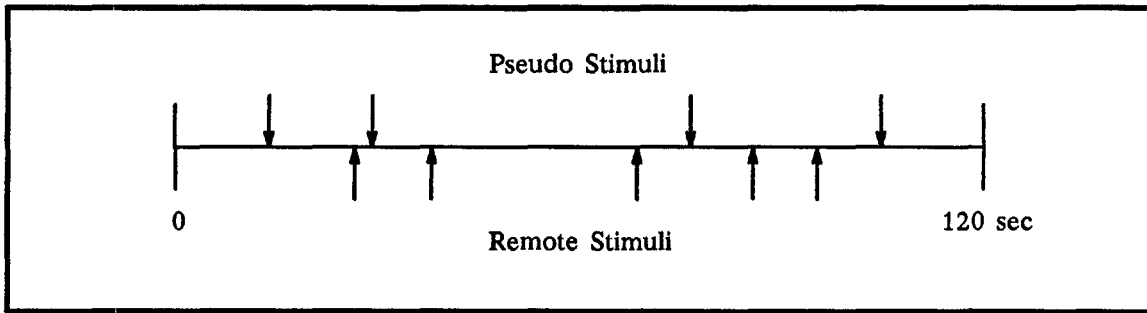


Figure 1. Schematic Timing Protocol—Single Run

c. Instructions to Viewers

In all sessions, the viewers were completely informed about the details of the experiments. Prior to their placement on the MEG table, they were shown the location of the RS display monitor, and were instructed to place their attention upon it or the sender during the session.

For some sessions, the viewer was instructed to press a fiber-optic-coupled button when he felt that he perceived stimuli. Each button press was marked in the data record. Button pressing was retained in this protocol as part of the conceptual replication.

d. Sensor-array Placement and Calibration

We selected the location for the sensor array by optimizing the viewer's response to direct visual stimuli. Inherent in this choice is an assumption that may not be valid: namely, that neurons participating in a reaction to RS are the same as those that respond to DS. The sensor locations were then marked on an acetate transparency to allow for accurate repositioning of the sensors in later sessions. One such placement (right occipital) is shown for viewer 002 in Figure 2.

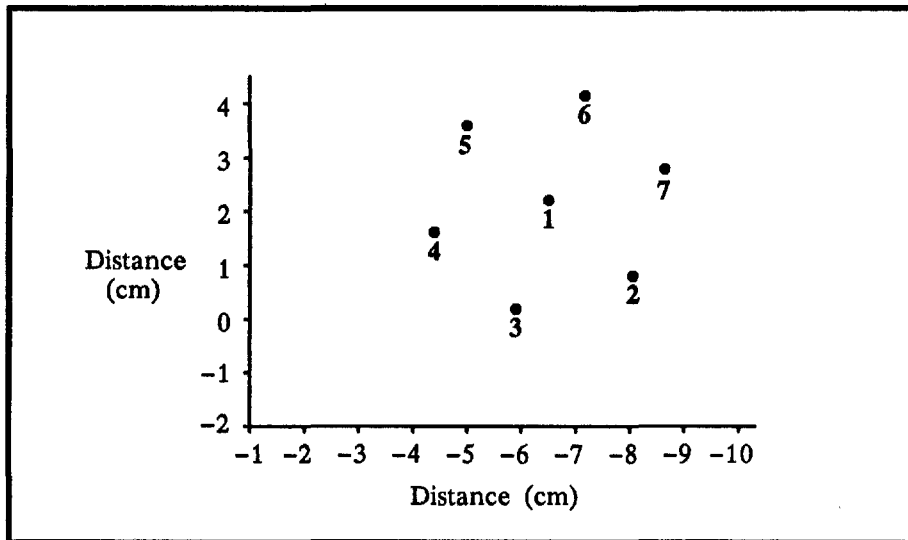


Figure 2. Sensor Position Relative to the Inion (0,0) for Viewer 002

For a calibration, the viewer was fitted with a spandex cap with grid marks aligned with his inion, nasion, and earlobes (i.e, head-centered coordinate system). The viewer was then placed as comfortably as possible on an observation table beneath the MEG. He must lie face down and look through a hole in the table to view the DS via a system of mirrors. These stimuli were displayed by a projector located outside the entrance to the shielded room. The sensors of the MEG were lowered from above to touch his head over the right occipital lobe. In this configuration, the sensor array was moved at the end of 30 DS to a position that optimized his response to the DS. Once found, the array position was marked on the cap for subsequent repositioning.

e. Sequence of Events for a Session

The following is the schedule of events for a session:

- Collect approximately 10 minutes of background data with no viewer or sender present and the MEG in full operation.
- Isolate the sender with the stimulus display device.
- With the viewer on the table, position the sensor array at the calibration point.
- At time = 0, start the monitoring of data with computer-generated trigger. Data are collected the entire 120 seconds at a rate of 200 samples per second.
- At time < 120 seconds, present 9 to 15 remote and 9 to 15 PS to the sender.
- At time > 120 seconds, allow the viewer to relax for about 2 to 5 minutes without leaving the table. This break generally consists of the sender entering the shielded room to engage the viewer in conversation.
- Collect nine additional runs with the same procedure while the viewer remains positioned on the table under the MEG.

C. Data Analyses

If our initial assumption about sensor positioning is true, and if the earlier results are replicated, we expect to see a change in alpha production as a result of the RS. We might also expect an evoked response similar to visual ERFs. Figure 3 is an idealized illustration of these expected results in the time-series data.

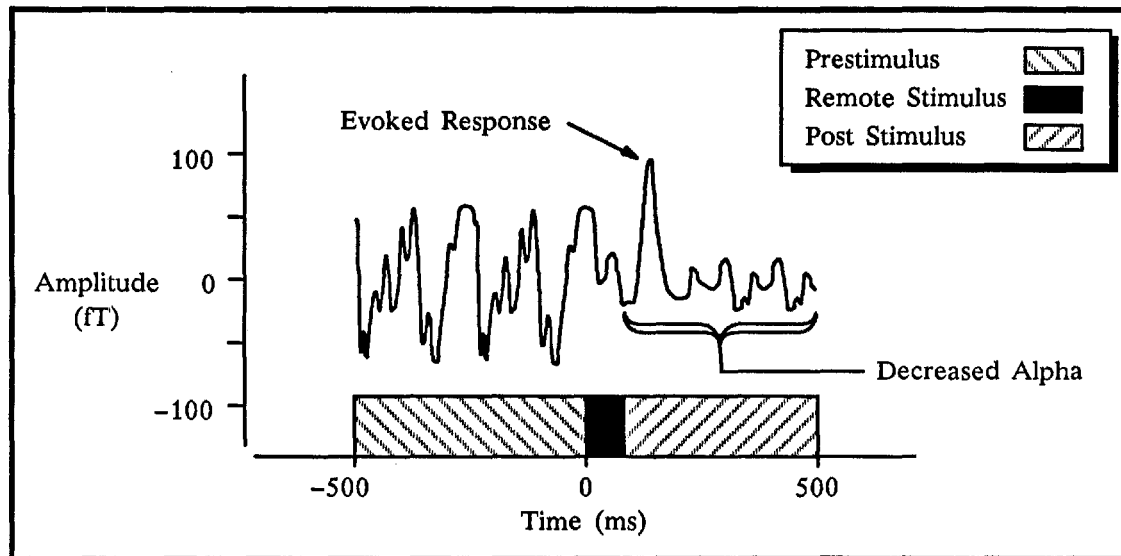


Figure 3. Idealized Results for a Single Stimulus

For each session, the following was computed for each RS and PS, respectively:

- (1) Five hundred ms of pre- and post-stimulus time-series data were separately detrended and filtered (40 Hz lowpass).
- (2) The power spectrum was computed for each 500-ms pre- and post-stimulus period.
- (3) The relative phase change of the dominant alpha frequency from pre- to post-stimulus period was computed as the arctangent of the ratio of the imaginary and real component of the transfer function. The transfer function is defined as the ratio of the FFT of the post-stimulus period divided by the FFT of the pre-stimulus period.
- (4) One thousand ms of time-series data (i.e., 500 ms pre- and post-stimulus) was separately detrended and filtered (40 Hz lowpass).

In addition, the following averages were computed across all RS and PS, respectively:

- (5) The average power pre- and post-stimulus.
- (6) The root-mean-square (RMS) average phase shift.
- (7) The 1000-ms time average of the pre- and post-stimulus periods taken as a single record.

- (8) The "power spectra" of the pre- and post-stimulus time averages were computed. (We recognize that a power spectrum of a time average is not an accurate representation of the average power spectrum, however it is an indicator of phase shift.)

D. Monte Carlo Calculations

The analysis of CNS activity has always been problematic, because alpha bursts lasting from 0.1 to a few seconds occur at random intervals. From a statistical point of view, the data fail to satisfy at least two underlying assumptions of the usual statistical methods (e.g., ANOVA and MANOVA). Most standard statistical tests assume that all samples of the data are independent. MANOVA can be configured to remove this particular assumption, nonetheless, it and the other tests assume that the process under study is stationary; that is, whatever the statistical properties are, they remain constant over time. In other words, the measured properties should not depend upon when the activity is sampled. CNS time series data do not satisfy either of these assumptions.

To avoid these difficulties, and to obtain probability estimates of the observed RMS phase shifts, we adopted a simple Monte Carlo approach. In the usual statistical analysis, the phase shift is compared to an ideal distribution, or its likelihood of occurrence is computed using some nonparametric technique. Both techniques attempt to determine the degree to which the observed phase shift is exceptional, given the universal set of all possible data. The Monte Carlo method that we used, however, can only determine the degree to which the observed phase shift is exceptional, given the available data sample.

The general Monte Carlo procedure is as follows:

- (1) Using the same timing algorithm to create the original RS, generate N sets of M stimuli, where M is the number of original RS.
- (2) For each pass ($1 \dots N$), compute the RMS phase shift averaged over M remote stimuli.
- (3) Sort the resulting N values to form the RMS phase shift distribution in the given data sample.
- (4) Compute the probability that the observed value would be as large (or larger), given a repeated random sample of the data. Note that this p-value is *not* the probability that the measure is as large, given a different data sample.

We have used this technique to compute p-values for the RMS phase shifts throughout this report.

III RESULTS

Eight viewers (002, 007, 009, 372, 374, 389, 454, and 531) from SRI International participated in the effort. Viewers 002, 009, 372, and 389 were experienced, with strong track records. Viewers 007, 374, and 531, had not previously participated in remote viewing experiments. Viewer 454 had participated in novice remote viewing training and has produced significant evidence of remote viewing ability.

A. Calculations

To illustrate the reduction of the raw data, we use the 25 September 1988 session from viewer 002.

Figure 4 shows the time average over all RS of the amplitude of the magnetic CNS activity of viewer 002's response to RS. The data from all seven sensors are displayed in a pattern that is similar to the physical sensor array. Each sensor is labeled in a highlighted box. The number of stimuli comprising the average (118) is shown in the key. The onset of the 100-ms stimulus is represented at *time* = 0, so negative time represents the pre-stimulus period and positive time represents the post-stimulus period. The total time period shown is 1 second. Because the stimuli are at random times relative to any uncorrelated CNS activity, averaging has reduced the amplitudes shown in Figure 4 by \sqrt{n} , where *n* is the number of stimuli. Sensor 7 shows a clear change from a slow, regular alpha rhythm during the pre-stimulus period, to one of higher frequency, post-stimulus.

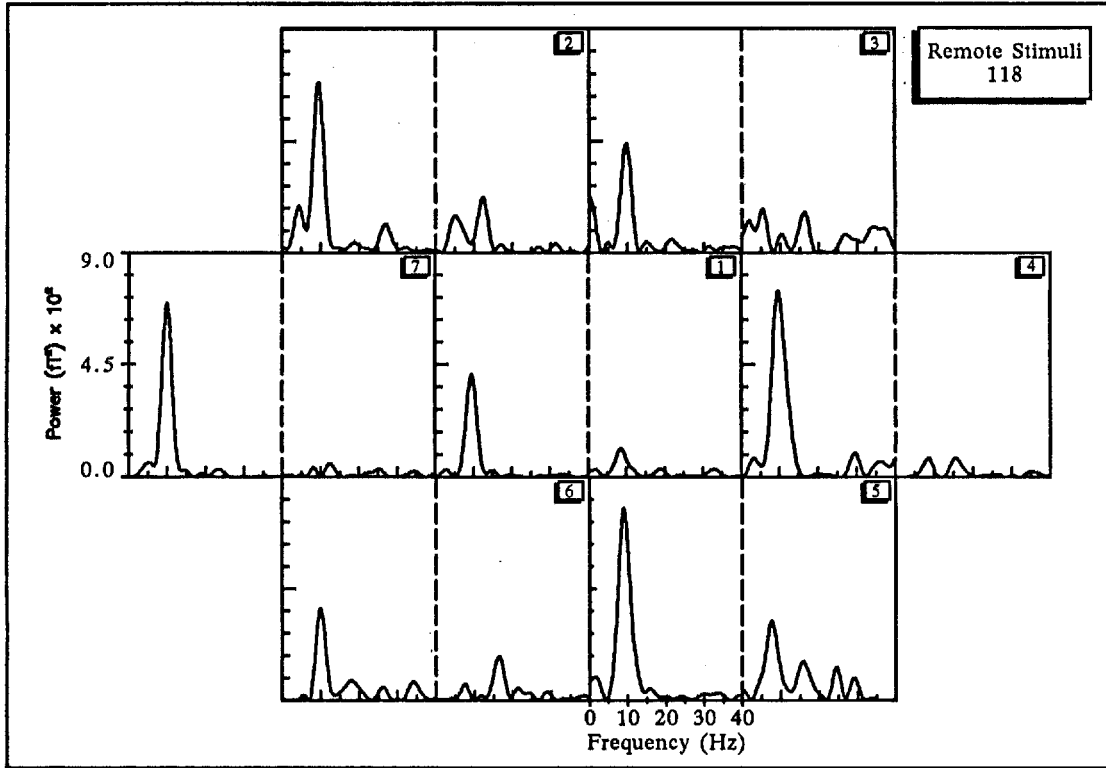


Figure 5. Viewer 2: Date 8/25/88: Session 1: Power of Time Average

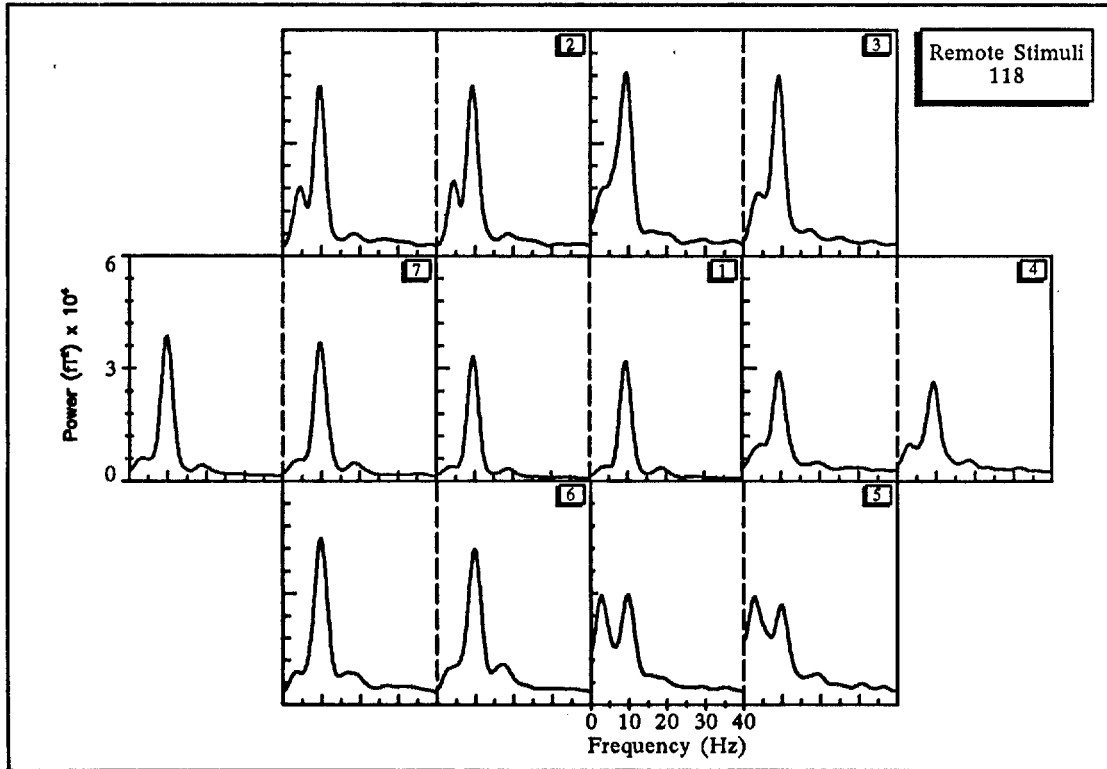


Figure 6. Viewer 2: Date 8/25/88: Session 1: Average Power

Figure 7 shows the ratio of the post- to pre-stimulus power. A dashed horizontal line is shown to indicate a gain of 1 (i.e., no change across the stimulus boundary). In this example, there is little change of CNS power across the stimulus boundary throughout the frequency range.

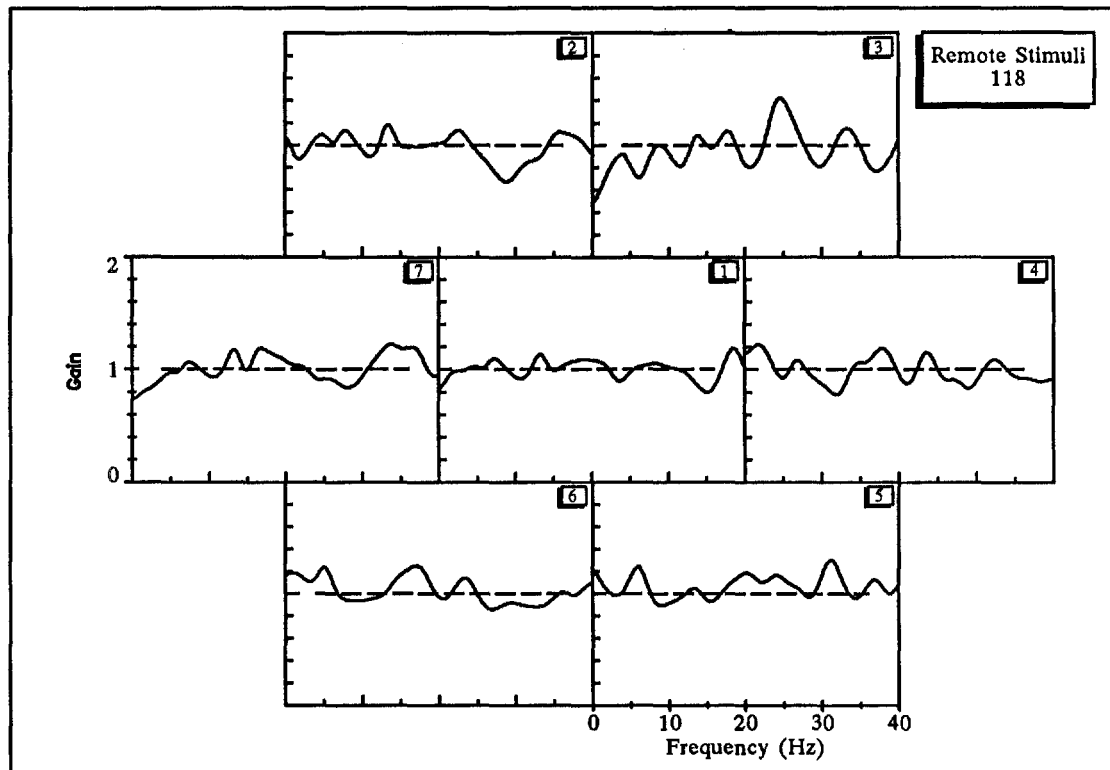


Figure 7. Viewer 2: Date 8/25/88: Session 1: Average Power Gain

Because a time average is sensitive to relative phase and a power spectrum is not, these data suggest that a relative phase shift occurs between pre- and post-stimulus periods. Figure 8 shows the RMS phase shift for all sensors. As was the case for the time-series data, the RMS average was computed over $n=118$ RS.

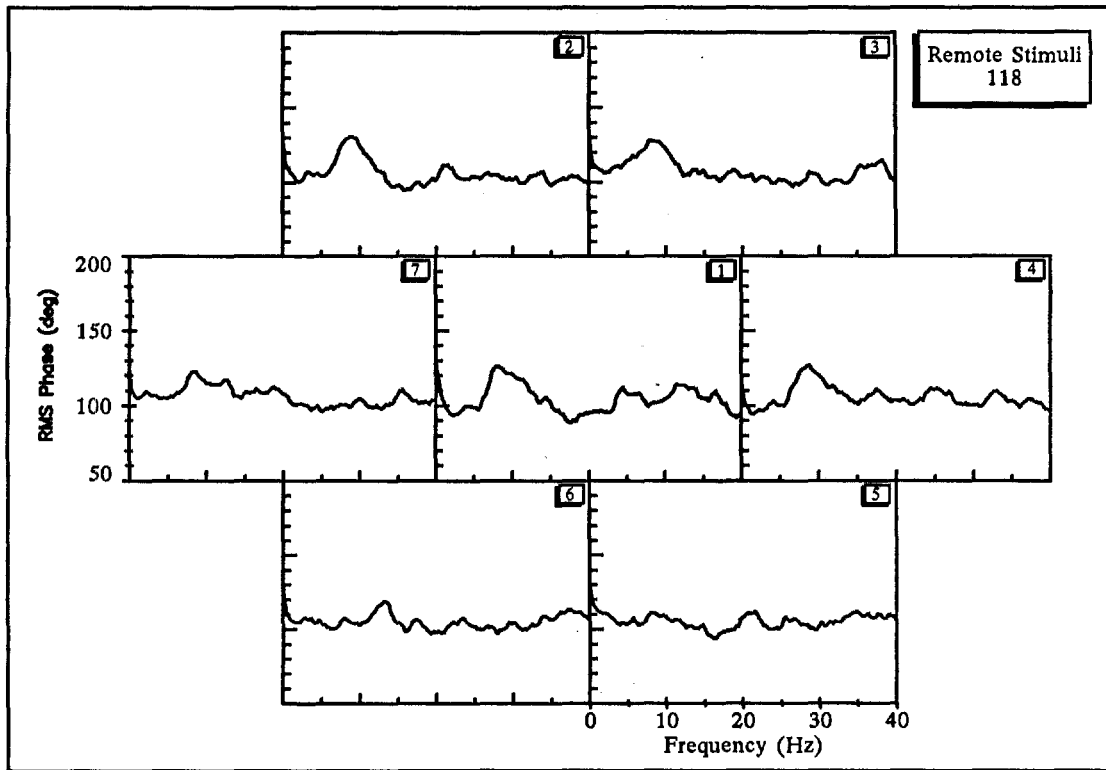


Figure 8. Viewer 2: Date 8/25/88: Session 1: RMS Phase

At this point we are unable to determine if the variations seen in Figures 4 through 8 are meaningful. Toward that end, the identical quantities for the PS are shown in Figures 9 through 13. The "power" of the time averages for the remote stimuli differ markedly from those of the PS spectra (Figures 5 and 10). Figure 14 shows an additional way of displaying this difference. The difference between remote and pseudo stimuli RMS phase shift is shown as a function of frequency (0 to 40 Hz).

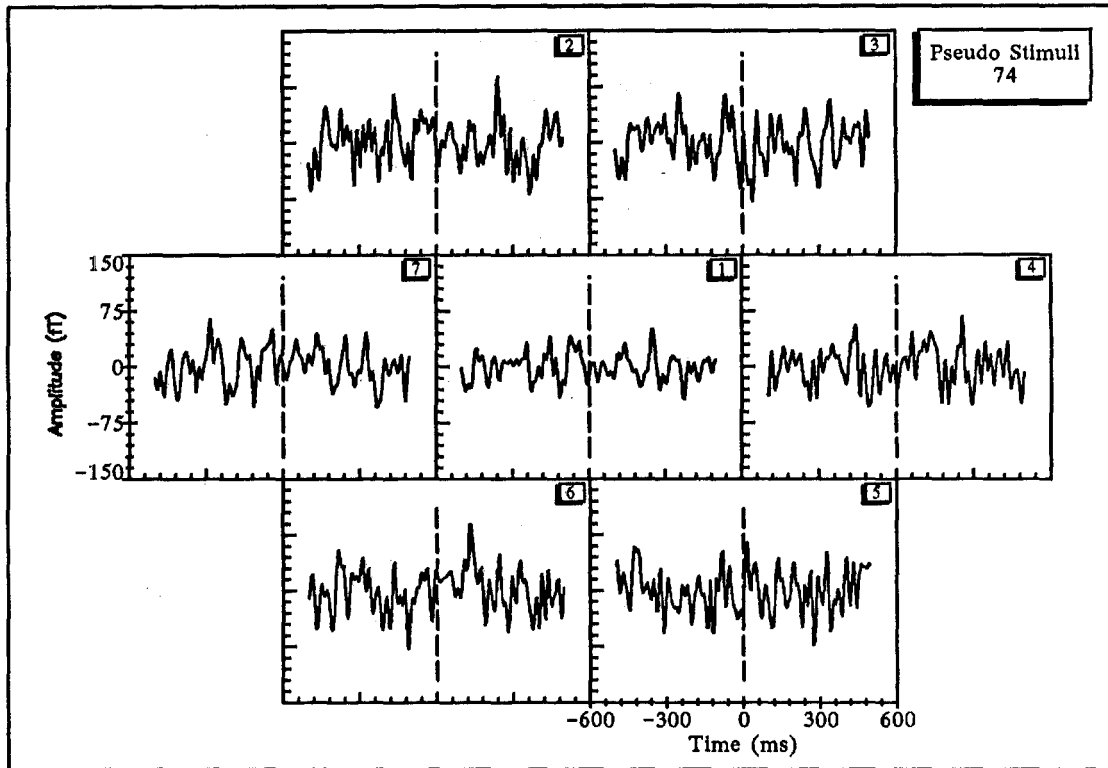


Figure 9. Viewer 2: Date 8/25/88: Session 1: Time Average

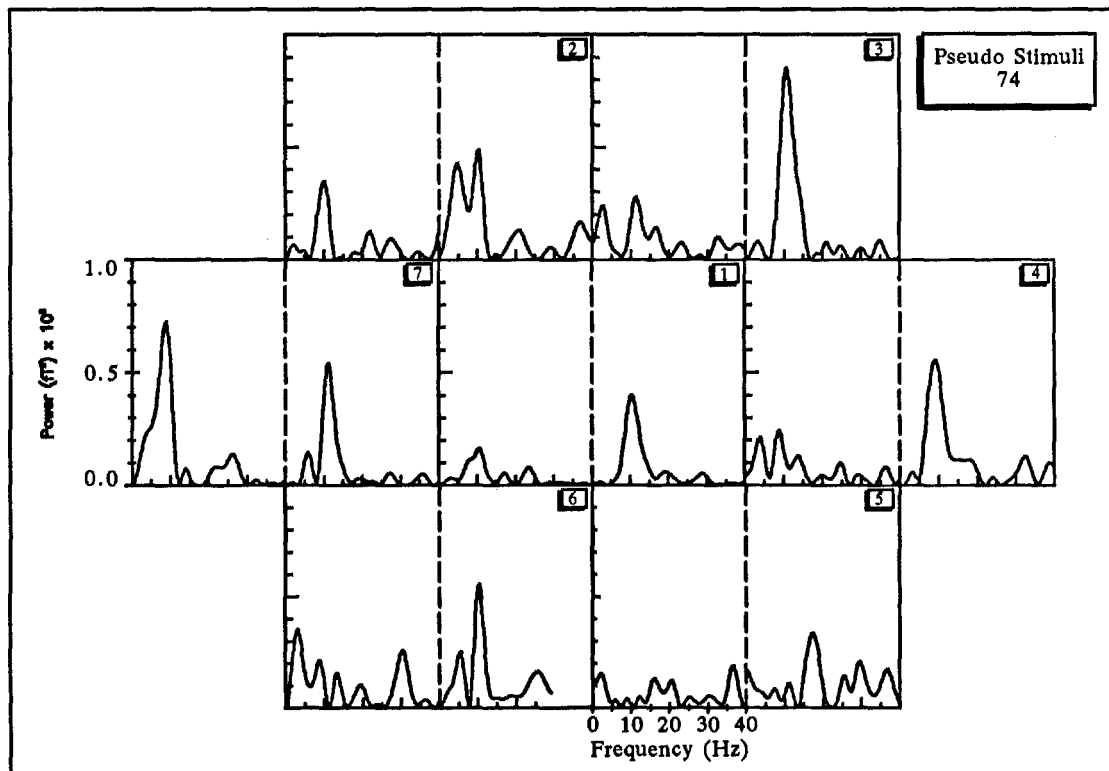


Figure 10. Viewer 2: Date 8/25/88: Session 1: Power of Time Average

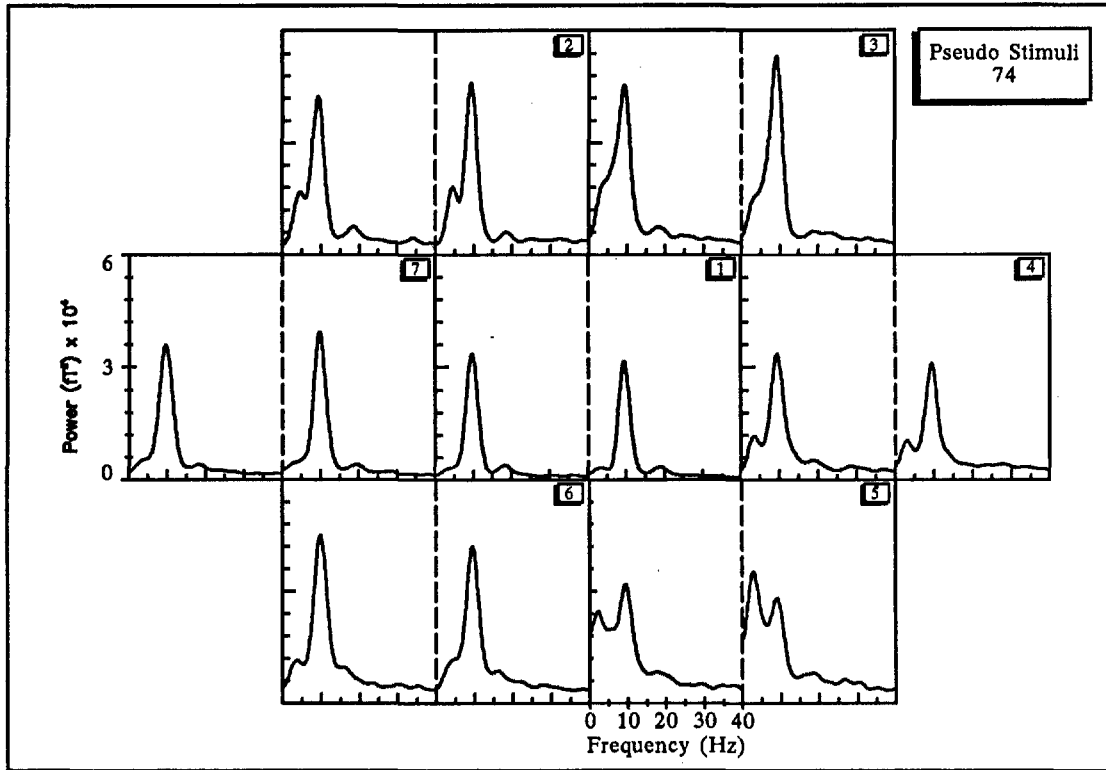


Figure 11. Viewer 2: Date 8/25/88: Session 1: Average Power

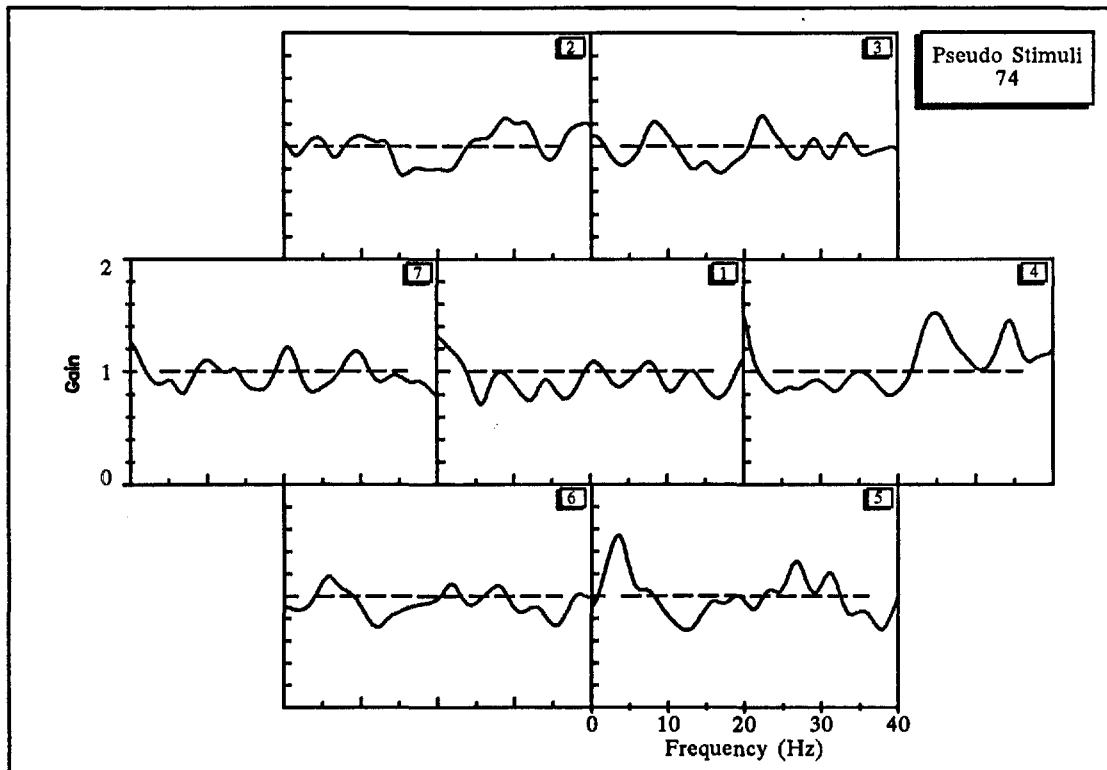


Figure 12. Viewer 2: Date 8/25/88: Session 1: Average Power Gain

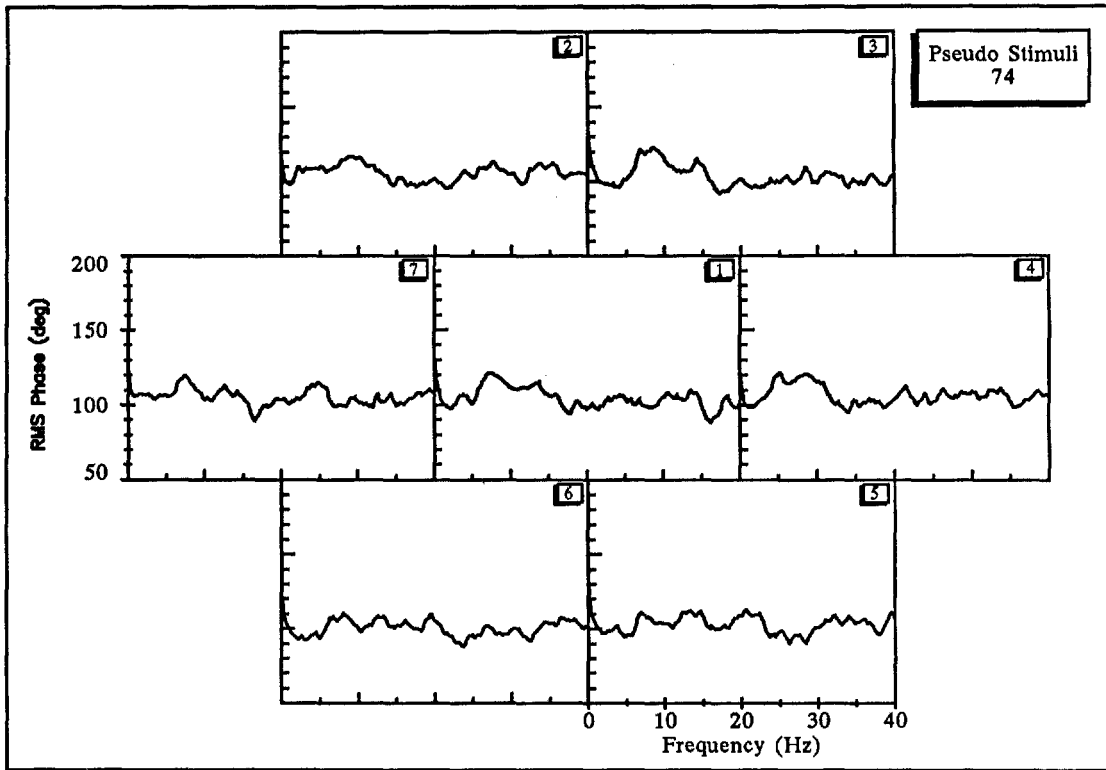


Figure 13. Viewer 2: Date 8/25/88: Session 1: RMS Phase

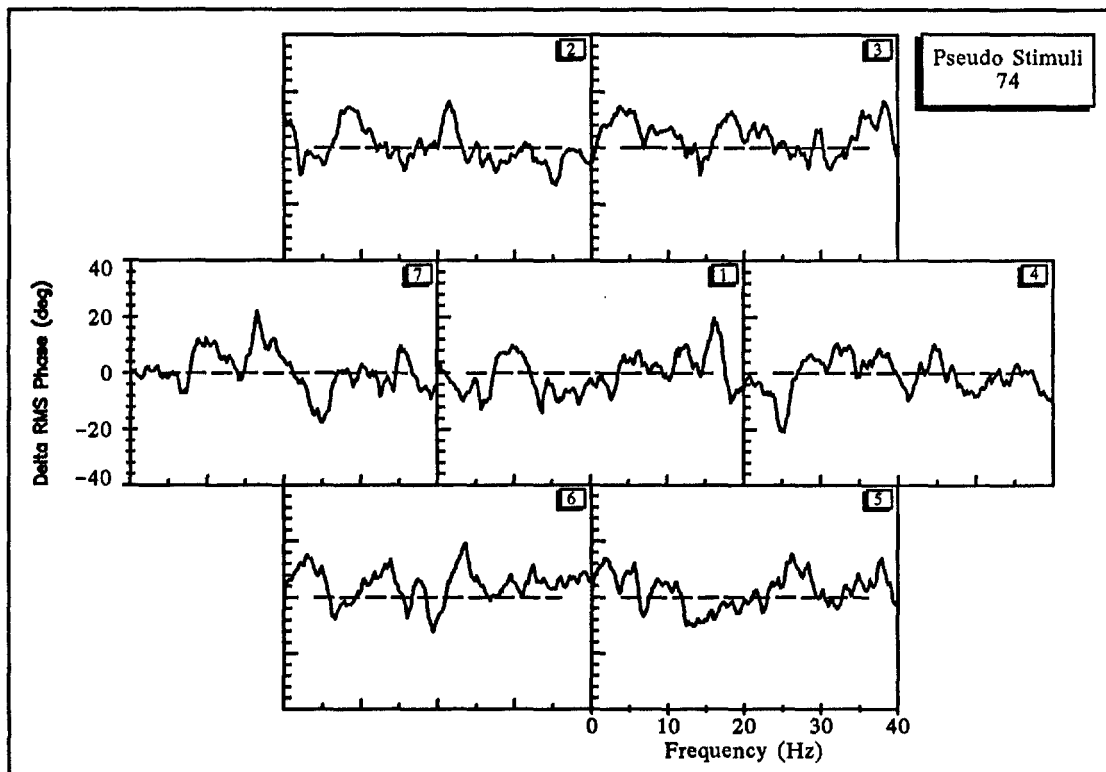


Figure 14. Viewer 2: Date 8/25/88: Session 1: RMS Phase Difference (rs-ps)

B. Monte Carlo Estimates of Significance

To determine if the changes that are seen qualitatively are exceptional, we analyzed the data by the Monte Carlo procedure outlined in Section II.D. We simulated the RS by generating 500 sets of Monte Carlo stimuli using the same random timing algorithm and number as in the original data. For each set, the RMS phase was calculated as described in Section II.C. The resulting 500 Monte Carlo RMS phases were sorted as a descending array, and the fraction of phases equal to or larger than the observed RS value was represented as a p-value. (The p-value is bounded on the low end by 1/500.) Figure 15 shows a histogram of one such Monte Carlo run, again using the data from viewer 002 as an example. The values of the RMS phase for the remote and pseudo stimuli are marked by vertical lines (see the key in Figure 15).

In accordance with the earlier study⁶ in which we observed changes in alpha power, we established a single criterion for the selection of a sensor for analysis: the pre-stimulus average alpha power above background is larger than it is in any other sensor. Table 1 shows the viewer identification, date, sensor chosen for analysis, and the p-value (as defined above) for the RMS phase shift for the remote and pseudo stimuli, respectively.

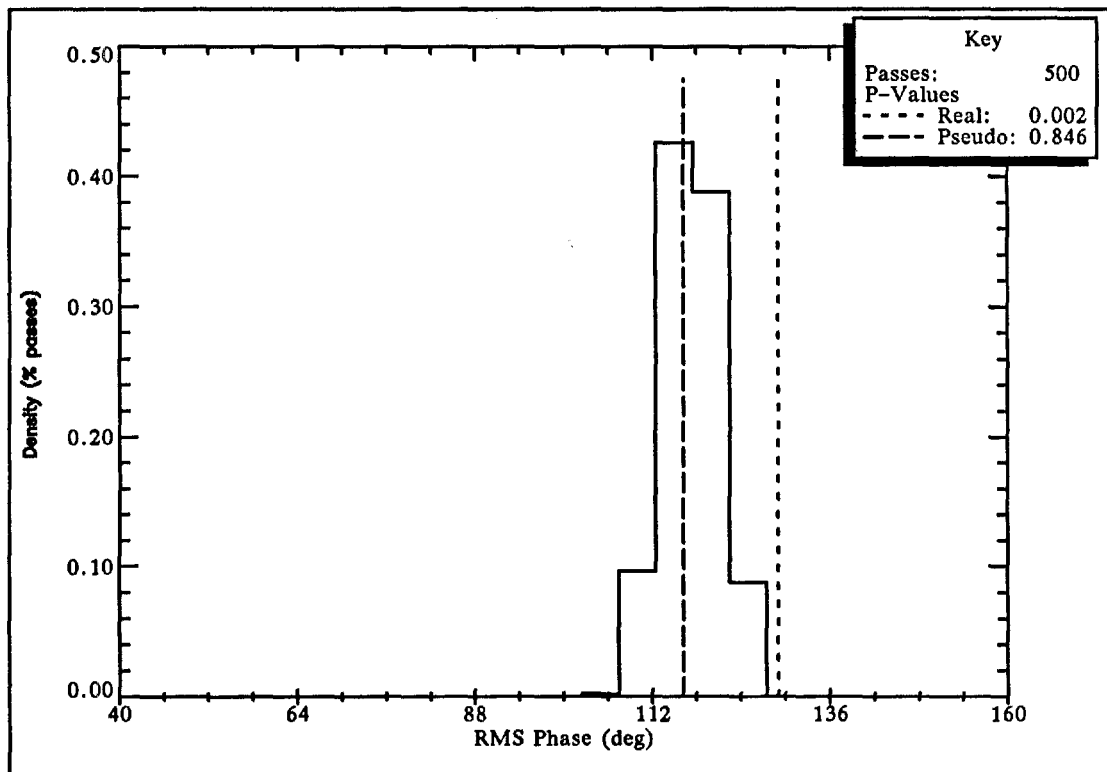


Figure 15. Viewer 2: Date 8/25/88: Session 1: RMS Phase: Sensor: 2 rs = 118

Table 1

Results of Monte Carlo Calculation for RMS Phase

I.D.	Date	Sensor	P-Value (1-tail)		Z-Score (2-tail)	
			Remote	Pseudo	Remote	Pseudo
009	06/24/88	6	0.650	-	-0.524	-
002	08/25/88	2	0.002	0.848	2.653	0.513
	08/26/88	6	0.904	0.966	0.871	1.491
372	10/19/88	7	0.094	0.168	0.885	0.423
374	03/29/89	6	0.154	0.810	0.501	0.305
007	03/29/89	7	0.970	0.180	1.555	0.358
389	05/23/89	4	0.288	0.040	-0.191	1.405
	05/24/89	5	0.260	0.016	-0.050	1.852
	05/25/89	4	0.120	0.922	0.706	1.011
531	05/24/89	4	0.814	0.134	0.274	0.619
454	05/25/89	4	0.732	0.052	-0.090	1.259

The p-values shown in Table 1 are all single tailed (i.e., the area in the upper tail). Because the distribution of means is approximately normal, we have converted the empirical p-values to their respective two-tailed z-scores. If the p-value was less than 0.5, the z-score shown in Table 1 was computed from the inverse normal distribution assuming a p-value twice the one shown. If the p-value was more than 0.5, we subtracted it from 1.0, doubled the result, and computed the z-score as above. To test the null hypothesis that the combined RS phase shifts are characteristic of the data, we computed a standard Stouffer's Z (Z_s) for the 11 sessions shown in Table 1. There is statistical evidence that the data within ± 0.5 seconds of the RS are *not* characteristic of the data at large ($Z_s = 1.99$, $p \leq 0.024$, *effect size* = 0.599). Similarly, the combined statistic for the PS indicates that these data are also *not* characteristic ($Z_s = 2.92$, $p \leq 0.002$, *effect size* = 0.924). Therefore, there appears to be some statistical anomaly associated with the RMS phase shifts for both stimuli types.

C. Results: Button Presses

In the early SRI study⁶, significant changes in alpha production were observed in response to an RS. The statistical evidence, however, did not indicate that the viewer was able to recognize an RS cognitively (i.e., the viewer's button presses relative to the RS did not exceed mean chance expectation).

In the current experiment, viewers 002, 009, and 372 were asked to press a button whenever they "perceived" an RS. The total number of stimuli during a session of 10 runs was not known in advance because of the randomization procedure. The null hypothesis is that the probability of a time interval having a stimulus is the same for those intervals with a button press as for those without a button press. In other words, the presence or absence of a stimulus is independent of the presence or absence of a button press. We tested this null hypothesis to determine if a viewer is cognitively aware of the RS.

In Table 2, the fractional hitting rate is $p_1 = A/(A+B)$, and the fractional missing rate is $p_2 = C/(C+D)$. The total number of 1-second intervals is $N = (A+B+C+D)$, and the total stimulus rate is $p_0 = (A+C)/N$.

Table 2

Data Schema for Interval Conditions

		Stimulus	
		Yes	No
Response	Yes	A	B
	No	C	D

Then the following statistic is approximately normally distributed with a mean of 0 and a variance of 1 under the null hypothesis:

$$z = \frac{(p_1 - p_2)}{\sqrt{p_0(1 - p_0)\left(\frac{1}{(A+B)} + \frac{1}{(C+D)}\right)}}$$

Table 3 shows N , p_0 , p_1 , p_2 , z , p-value, and the effect size, r , for the three sessions for which button-press data were collected. As in the earlier SRI study, there is no indication that the viewers were cognitively aware of the RS.

Table 3

Button Pressing Results

Viewer	N	p_0	p_1	p_2	z	p	r
002	1210	0.167	0.198	0.164	0.951	0.163	0.027
009	1280	0.091	0.068	0.094	-0.978	0.836	-0.027
372	1089	0.157	0.119	0.160	-0.996	0.840	-0.030

IV DISCUSSION AND CONCLUSIONS

We have found statistical evidence that the relative phase shift from -0.5 to 0.5 seconds of an RS are *not* characteristic of the data at large ($Z_s = 1.99, p \leq 0.024, \text{effect size} = 0.599$). The combined statistic for the PS indicates that the relative phase shift from -0.5 to 0.5 seconds of a PS are also *not* characteristic of the data at large ($Z_s = 2.92, p \leq 0.002, \text{effect size} = 0.924$). Averaged across all viewers, the magnitude of the results, as indicated by their effect sizes of 0.599 and 0.924, respectively, is considered robust by accepted behavioral criteria defined by Cohen.^{9*}

A. Root-Mean-Square Phase

Searching for a change of phase as a result of an RS is a natural extension of results quoted in the literature. For example, Rebert and Turner⁶ report an example of photic driving (i.e., an extreme example of phase locking) at 16 Hz. In their work, a subject was exposed to a 16-Hz visual DS randomly balanced with no stimulus during 4-second epochs. The average power spectra showed approximately 10-Hz alpha activity during the no-light epochs, and a strong 16-Hz and no 10-Hz peak during the 16-Hz epochs.

One interpretation of their result is that the alpha rhythm was blocked, and the CNS "locked" on to the flashing stimulus. Eason, Oden, White and White,¹⁰ report a phase-shift phenomenon when a rare stimulus, which is random relative to the internal alpha activity, is presented as a DS:

"...when a stimulus flash is presented, the resulting primary evoked response acts as a trigger stimulus which temporarily synchronized a certain percentage of the neural elements normally under the influence of an internal pacemaker. ... Desynchronization of the elements participating in the evoked response would occur as the elements are brought back under the influence of an internal pacemaker or are affected by neurons not involved in the response."

In other words, the internal alpha is momentarily interrupted by an external stimulus, and, in the absence of continuing external stimuli, returns back to its original frequency, but at a random phase relative to its pre-stimulus state.

To understand what would be expected in our experiment for the distribution of RMS phases during the Monte Carlo simulations, we examine a hypothetical case. Suppose that the

* Values of 0.1, 0.3, and 0.5 correspond to small, medium, and large effects, respectively.

viewer's alpha activity was a continuous wave at a single frequency. A phase change is computed between 500 ms before and 500 ms after each Monte Carlo "stimulus." Therefore, regardless of the entry point, the relative phase change would be zero, and the RMS phase over many such "stimuli" would also be zero.

Real alpha activity, however, is not continuous. Rather, it appears in bursts lasting from 100 to 5000 ms. Random Monte Carlo "stimuli" would sometimes occur within such bursts and sometimes near the edges. Thus, we would expect a nonzero RMS phase over many such "stimuli," but the individual relative phases would not be uniformly distributed. Depending upon the viewers' alpha characteristics, the distributions would be enhanced near zero RMS phase.

If we assume that Eason, et al., are correct, and that a phase shift is expected as a result of an RS, then the expected distribution of RMS phases is uniformly distributed on $[-\pi, \pi]$. In this case, the phase change is related to the relative timing between the external stimulus and the internal alpha—a completely random relationship. Thus, the variance of the RMS phases in the experimental condition should be larger than those computed during the Monte Carlo runs. Figure 16 is a schematic representation of these models.

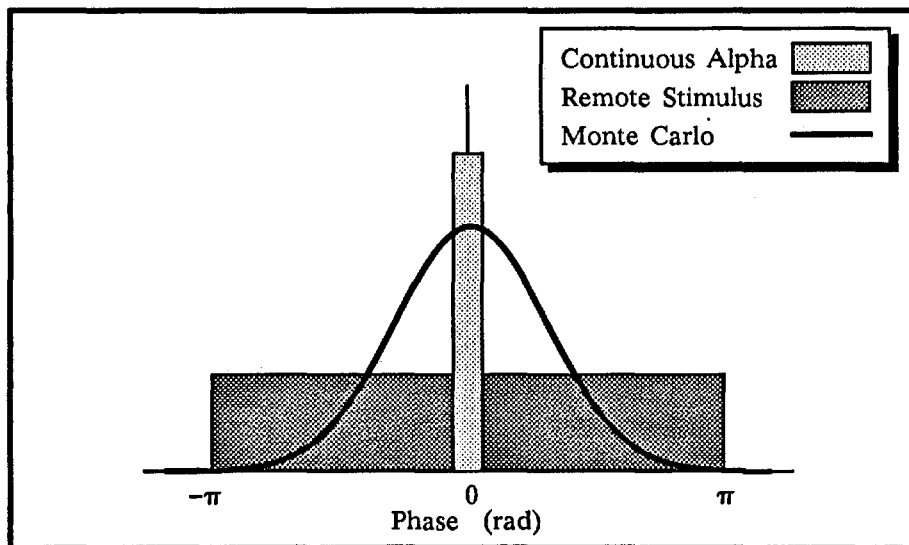


Figure 16. Idealized Distributions for Relative Phase Shifts

As a first step in testing these models, we computed the expected variance for the RMS phase, given that the individual phases are uniformly distributed on $[-\pi, \pi]$. Using a Taylor Series expansion for RMS phase, the variance is given by:^{11*}

* We thank Professor Jessica M. Utts, Statistics Department, University of California, Davis, California, for suggesting this approach.

$$\sigma_y^2 = \frac{\frac{3}{45}\pi^2}{n} \left[1 - \frac{1}{30n} \right] \text{ (rad}^2\text{) , or}$$

$$\approx \frac{2160}{n} \text{ (deg}^2\text{),}$$

where n is the number of individual phases.

Table 4 shows the viewer identification, the two-tailed z-score from Table 1, the number of RS, the theoretical variance for the RMS phase, the observed variance from the Monte Carlo runs of 500 passes each, and the X^2 and its associated p-value for a variance-ratio test.

Table 4

Comparison Between Monte Carlo Phases and Theory

I.D.	Z-Score (RS)	Number of RS	Variance of RMS Phase		X^2 df = 499	P-Value
			Theoretical	Observed		
009	-0.524	96	22.50	25.46	564.6	0.978
002	2.653	118	18.31	13.63	371.5	4.9×10^{-6}
	0.871	76	28.42	24.43	428.1	0.010
372	0.885	90	24.00	23.25	483.4	0.316
374	0.501	102	21.18	18.64	439.2	0.025
007	1.555	93	23.23	18.66	400.8	4.6×10^{-4}
389	-0.191	97	22.27	23.35	523.2	0.780
	-0.050	92	23.48	22.29	473.7	0.214
	0.706	98	22.04	20.22	457.8	0.093
531	0.274	101	21.39	21.05	491.1	0.408
454	-0.090	52	41.54	40.48	487.3	0.363

Combining the X^2 across all 11 sessions gives an overall significant result ($X^2 = 5121.5$, $df = 5489$, $p \leq 0.0002$). This indicates that the Monte-Carlo-derived variances are significantly smaller than the theoretical variances based on uniformly distributed phases. The two viewers who demonstrated the largest z-scores (002 and 007) also show sharply reduced Monte Carlo variances. This may indicate that the RS are the source of increased variance.

Figure 17 shows the distribution of phases for the RS and Monte Carlo stimuli. While the RS distribution is enhanced near ± 180 degrees and suppressed near 0 degrees compared to the Monte Carlo distribution, the differences are small ($X^2 = 10.62$, $df = 8$, $p \leq 0.224$) and, therefore, the

random-phase model does not appear to be a good fit to the data for viewer 002 on his 25 September session.

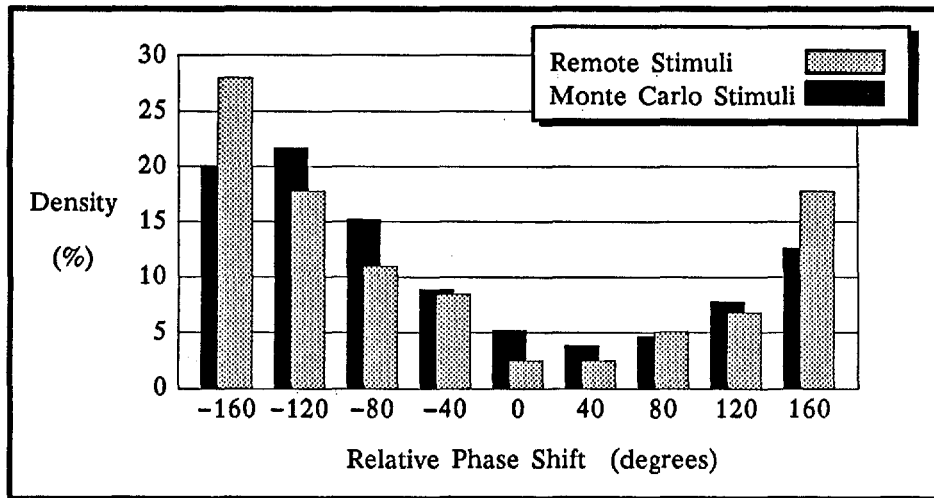


Figure 17. Phase Distributions for Viewer 002: 8/25/88

Figure 18 shows the same distributions for viewer 007. In this case, the RS distribution is nearly uniform on $[-180, 180]$ degrees, but it differs only slightly from the Monte Carlo distribution ($X^2 = 9.47, df = 8, p \leq 0.304$). Thus, the random-phase model is not a good fit these data, either.

From the data shown in Table 4, we see that the X^2 indicates significant overall differences between the theoretical and observed phase distributions. However, Figures 17 and 18 show that the differences between RS and Monte Carlo distributions are small. It is most probable, therefore, that the RS coupling to the CNS is weak, in general, and that the position of the sensor array is not necessarily optimized to sense the phase changes.

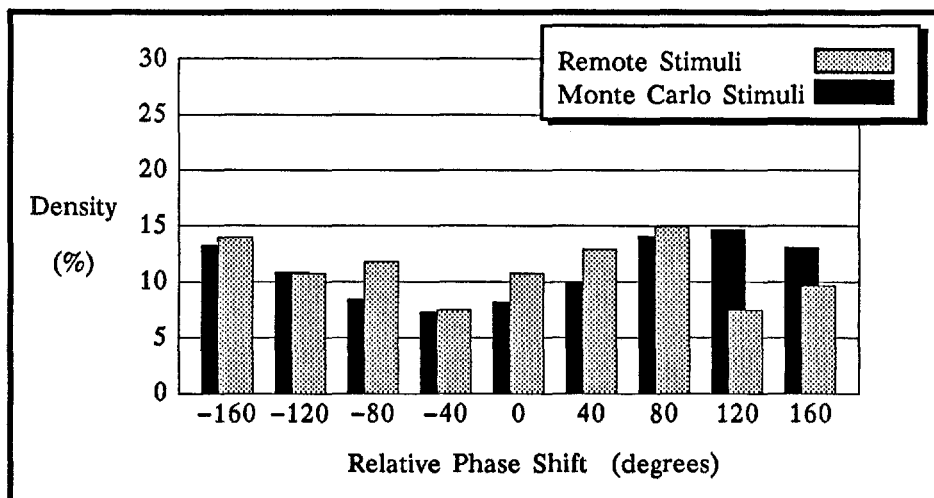


Figure 18. Phase Distributions for Viewer 007: 3/29/89

B. Viewer Dependencies

Viewers 002, 009, and 372 have produced consistent remote viewing results for many years—since 1972 for viewers 002 and 009, and since 1979 for viewer 372. Viewer 389 is a recent addition, and has produced examples of excellent remote viewing in the only experiment in which he has participated; however, he has produced significant results in another laboratory. Whereas viewer 002 produced the largest z-score ($Z_s = 2.653$), viewer 009 produced the smallest ($Z_s = -0.524$). The combined effect size for the experienced viewers is 0.621, and is 0.559 for the inexperienced viewers. The difference is not significant.

There are two considerations that prevent drawing conclusions about the viewer dependence of the data. The number of independent samples is small, but the most compelling argument against drawing conclusions is that placement of the sensor array is a seriously confounding factor. As stated in Section II, we positioned the array in a location that maximized the response to a DS. This may not be the appropriate positioning for everyone. Indeed, it might not be optimal for anyone.

To determine if there were any “obvious” spatial dependencies that might indicate a more optimal array placement, we computed a complete set (all sensors) of Monte Carlo distributions for one session for viewer 002. Figure 19 shows the single-tailed p-values for the RMS phases for the RS and PS. They are displayed in the standard sensor-array configuration. The pattern for the RS suggests that a more optimal positioning of the array would be in the sensor 2-7 direction as indicated by an arrow in Figure 19.

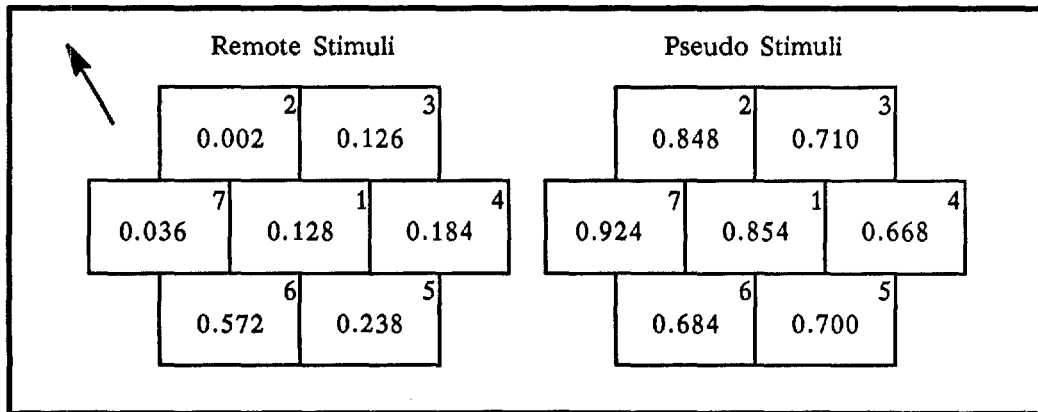


Figure 19. Phase p-values for Viewer 002: 8/25/88

C. Pseudo Stimuli

It was initially thought that the PS would act as a within-run control. The results indicate, however, that there was, on the average, a larger response to the PS than to the RS. While the difference was not significant, it is important to note that both of the responses are considered statistically robust (effect sizes of 0.599 and 0.924 for the RS and PS, respectively). A number of

viewers' responses appear to produce phases on opposite sides of the Monte Carlo distributions (e.g., viewers 002 and 007), but there is no overall correlation between the RS and PS p-values.

A brief description of the hardware and software that is responsible for stimulus generation may help in understanding this outcome. The stimuli and their timing are initiated by an HP computer, but are controlled by an IBM PC. Each stimulus type has its own frame buffer within the PC. Our RS consists of a pattern of 1s and 0s that represent a sinusoidal grating in the center of an otherwise blank field. The PS pattern, a blank field that consists of all 0s, resides in a separate buffer. An interface board between the PC and a standard video monitor has its own internal frame buffer, which is automatically and continuously scanned at 30 Hz to provide a standard NTSC interleaved video signal. See Figure 20.

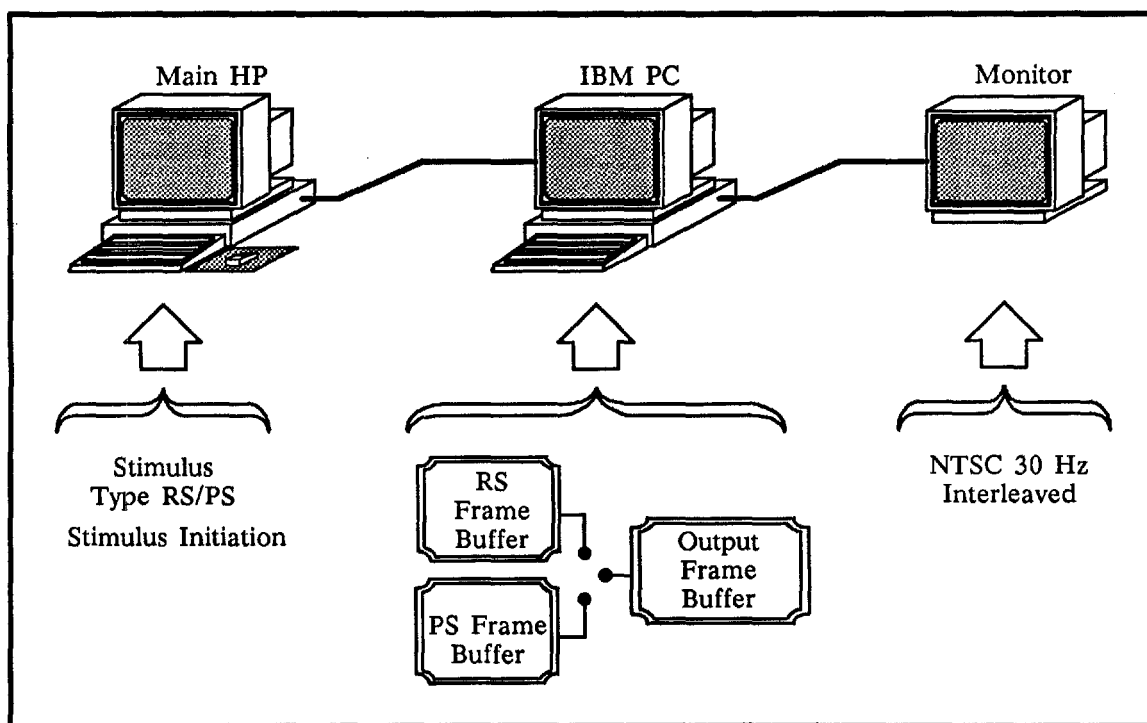


Figure 20 . Sequence of Events for Stimuli Generation

When the HP computer signals the PC to provide the appropriate stimulus, the following sequence of events are followed (see Figure 20):

- (1) Phase locked to 60 Hz, the interface frame buffer is loaded with a copy of the appropriate stimulus frame buffer (either RS or PS).
- (2) The interface board automatically sends this pattern interleaved at 30-Hz.
- (3) After a preset time, approximately 100-ms in our experiment, the PC resets the interface frame buffer to zero (blank screen), and waits until another stimulus signal is received.

At the video monitor, the PS are indistinguishable from the between-stimuli blank screens. At the PC, however, the PS are distinguishable from the blank screen background, because the PC must copy a frame buffer (albeit all 0s) into the output frame buffer.

In our experiment, the RS and PS results were statistically identical, and independently, both were significantly different from the Monte Carlo distributions. This raises the question as to what constitutes the target stimulus. Our result is unexpected given the target is considered to be what is displayed on the remote monitor.

It is conceivable that the internal activity of the PC, or its companion computer, is acting as an unintended target. If this were true, then there might be an electromagnetic (EM) coupling between the viewer's CNS and the internal electronic activity of the computers. It is well known that computers radiate EM energies at relatively high frequencies; for frequencies above 100 Hz, the shielded room is transparent. Analysis of the background runs (i.e., data collected in the absence of a sender or viewer) showed no EM coupling into the MEG electronics, it remains possible that the statistical effects we have seen are due to CNS responses to remote bursts of EM energy.

Let us *assume* that the overall RS and PS effects are meaningful. Since the PSs are *indistinguishable* at the monitor from the between-stimuli background but are *distinguishable* at the IBM PC, then the present experiment demonstrates that the source of stimuli is the IBM PC.

During the SRI/Langley Porter study in 1977, SRI developed an entirely battery operated stimulus generator as a special precaution against the possibility of system artifacts in the form of EM pickup. They reported significant CNS responses to remote stimuli, nonetheless.⁶ Therefore, it remains possible that we have observed an anomalous information transfer.

Before further research is conducted (see Section D below), it is important to measure the EM radiation patterns, and to see if they are of sufficient strength to be detected (by the appropriate hardware) in the shielded room.

By adjusting the PC program, the PS internal activity can be eliminated. It would be interesting to see if the similarity between the RS and PS results persists.

D. Recommendations for Further Research

Dr. C. C. Wood (current director of the Neuromagnetism Laboratory at LANL) and Dr. E. R. Flynn (former director) have provided the following recommendations for continued investigations. This abbreviated list of topics summarizes a day-long discussion with the SRI staff about the most promising directions for further research.

- (1) Search for neurophysiological mechanisms of remote viewing capability. Although the FY 1989 experiment produced strong suggestive evidence that remote viewing significantly alters the neuromagnetically recorded brain activity in the alpha (approximately 10 Hz) band, additional work is needed to develop measures of the effect that can be localized to specific brain regions by means of source localization models. This goal is particularly important for understanding the neural mechanisms of remote viewing. Does the effect involve activation of the visual structures that mediate normal vision? Or are additional structures involved?
- (2) Analyze neuromagnetic activity elicited by near-threshold stimuli in signal-detection tasks. In order to increase our understanding of how weak signals might influence neuromagnetic brain activity, we propose to compare the remote viewing data obtained in FY 1989 with that elicited by near-threshold stimuli in signal-detection tasks. For the behavioral data obtained in such tasks, a well-developed body of mathematical theory exists that will be of considerable value in distinguishing between aspects of brain activity elicited by weak signals and those related to subjects' perception of those signals.
- (3) Use advanced signal-processing techniques to assess changes in neuromagnetic activity induced by remote viewing. The FY 1989 results suggestive of remote viewing effects are based on spectral analysis of pre- and post-event time epochs. These analyses focused on alpha band activity because that activity was most obvious to visual inspection of the pre- and post-event epochs. In order to determine the optimal means of characterizing remote viewing effects, we propose to employ a variety of advanced signal processing algorithms, including nonlinear dynamic analysis, to achieve a more complete characterization of such effects.
- (4) Explore possible neurophysiological screening techniques for high-likelihood remote viewing capability. Anecdotal observations in conjunction with FY 1989 experiments suggest that some "calibrated" remote viewers may have unusually large magnetic responses to visual stimulation. To follow up this observation, we propose to compare magnetic responses of visual, auditory, and somatosensory stimulation in "calibrated" remote viewers, with matched controls, who demonstrate no remote viewing capability.

V ACKNOWLEDGMENT

The Cognitive Sciences Program staff appreciate the warm welcome provided by the staff of the Neuromagnetism Laboratory at LANL. In particular, we thank Dr. M. Oakley for assisting us with data collection and suggesting the phase model. Without the help of Dr. E. Flynn, the experiment could not have been conducted, and we thank Dr. C. Wood for providing promising directions for future research.

REFERENCES

1. Dean, E. D., *International Journal of Neuropsychiatry*, Vol. 2, p 439, 1966.
2. Tart, C. T., *International Journal of Parapsychology*, Vol. 5, p 375, 1963.
3. Duane, T. D., and Behrendt, T., *Science*, Vol. 150, p. 367, 1965.
4. Cavanna, R., Ed., *Psi Favorable States of Consciousness*, Parapsychology Foundation, New York, 1970.
5. Rebert, C. S., and Turner, A., "EEG Spectrum Analysis Techniques Applied to the Problem of Psi Phenomena," *Physician's Drug Manual*, Vol. 6, Nos. 1-8, pp 82-88, 1974.
6. Targ, R., May, E. C., Puthoff, H. E., Galin, D., and Ornstein, R., "Sensing of Remote EM Sources (Physiological Correlates)," Final Report, Project 4540, SRI International, Menlo Park, CA, 1977.
7. Sutherland, W. W., Crandall, P. H., Cahan, L. D., and Barth, D. S., "The Magnetic Field of Epileptic Spikes Agrees with Intracranial Localizations in Complex Partial Epilepsy," *Neurology*, Vol. 38, No. 5, pp 778-786, May 1988.
8. Aine, C. J., George, J. S., Medvick, P. A., Oakley, M. T., and Flynn, E. R., "Source Localization of Components of the Visual-Evoked Neuromagnetic Response," Neuromagnetism Laboratory, Life Sciences and Physics Divisions, Los Alamos National Laboratory, Los Alamos, NM.
9. Cohen, J., *Statistical Power Analysis for the Behavioral Sciences* (rev. ed.), Academic Press, New York, 1977.
10. Eason, R. G., Oden, D., White, B. A., and White, C. T., "Visually Evoked Cortical Potentials and Reaction Time in Relation to Site of Retinal Stimulation," *Electroencephalography and Clinical Neurophysiology*, Vol. 22, pp 313-324, 1967.
11. Rice, J. A., *Mathematical Statistics and Data Analysis*, Wadsworth & Brooks/Cole Advanced Books & Software, Pacific Grove, p 143, 1988.